

Feynman rules for effective Regge action

E.N. Antonov* and L.N. Lipatov†

Petersburg Nuclear Physics Institute, RU-188350 PNPI, Gatchina, St.Petersburg, Russia

E.A. Kuraev‡

Joint Institute for Nuclear Research, RU-141980 BLTP JINR, Dubna, Russia

I.O. Cherednikov§

*Joint Institute for Nuclear Research, RU-141980 BLTP JINR, Dubna, Russia and
Dipartimento di Fisica, Università di Cagliari and INFN-Cagliari, C.P. 170, I-90142 Monserrato (CA), Italy*

(Dated: January 27, 2020)

Starting from the gauge invariant effective action in the quasi-multi-Regge kinematics (QMRK), we obtain the effective reggeized gluon (R) – particle (P) vertices of the following types: RP , RPP , RRP , $RRPP$, $RPPP$, $RRPPP$, and $RPPPP$, where the *on*-mass-shell particles are gluons, or sets of gluons with small invariant masses. The explicit expressions satisfying the Bose-symmetry and gauge invariance conditions are obtained. As a comment to Feynman rules for derivation of the amplitudes in terms of effective vertices we present a “vocabulary” for practitioners.

PACS numbers: 12.38.-t, 12.40.Nn

I. INTRODUCTION

The problem of unitarization of the BFKL Pomeron is among the most urgent directions of investigations in phenomenology of strong interactions. The BFKL evolution is applied to describe the hadronic scattering amplitudes in the Regge regime $s \rightarrow \infty$, $s \gg -t$ determining the high-energy behavior of total cross sections of QCD processes [1]. Moreover, the BFKL (with the DGLAP) equation is used to resum the leading logarithmic contributions to the structure functions in deep inelastic scattering, and thus is relevant to the problem of gluon saturation at small Bjorken x_{Bj} , in particular, in connection with the rapid growth of the $F_2(x, Q^2)$ function observed at HERA [2].

In the leading logarithmic approximation, the BFKL equation gives the power-law rise of cross sections with energy that obviously violates the Froissart bound which guarantees the unitarity. In the literature, the two methods to overcome this problem are discussed: one suggests to take into account the multiple Pomeron exchanges in the leading logarithmic approximation, while the other consists in going beyond the leading logarithmic approximation and find a systematic method to take into account non-leading (NLO) corrections to BFKL.

A fruitful approach to study hadron processes at high-energy which is explored by both of these two methods is to try to re-formulate the complicated QCD dynamics in terms of some effective theory which is easier to solve in a given regime [15]. The idea to apply a two dimensional (in the impact parameter space) effective theory to study high-energy QCD amplitudes was proposed first in Ref. [16] where a two-dimensional sigma-model defined on the scattering transverse plane was formulated and the scattering amplitude was expressed in terms of the vacuum expectation value of two light-like Wilson path-ordered exponentials. Within this framework, the behavior of scattering amplitude, or structure functions, is described by the non-linear evolution equation with respect to shift of the Wilson operators from the light-cone. However, that approach was incomplete and suffered from certain shortcomings. Then, in the works by I. Balitsky [17], the high-energy scattering was considered by means of factorization in rapidity space within the shock-wave picture, and the gauge invariant effective action was proposed in terms of the corresponding Wilson lines. In this approach, the high-energy behavior is described by a non-linear evolution equation, now known as Balitsky–Kovchegov (BK) equation [17, 18]. The similar, to some extent, methods based on the renormalization group properties were developed in Refs. [7, 8]).

On the other hand, the most straightforward way to deal with the unitarization problem is to evaluate the non-leading contributions to BFKL. The explicit calculation of the NLO logarithmic corrections to the Pomeron intercept

*Electronic address: antonov@thd.pnpi.spb.ru

†Electronic address: lipatov@thd.pnpi.spb.ru

‡Electronic address: kuraev@thsun1.jinr.ru

§Electronic address: igor.cherednikov@jinr.ru; igor.cherednikov@ca.infn.it

have been performed in the fifteen-years old papers by L.N. Lipatov and V.S. Fadin [3] for one and two gluon production. The result was rather cumbersome and not convenient for numerical analysis. Nevertheless, it was realized that the next-to-leading corrections to the BFKL kernel are large enough and must be taken into account even at presently accessible energies [4–6].

In the present study, we deal with the effective approach proposed by L.N. Lipatov. It appears to be convenient and physically well-motivated to perform the systematic self-consistent study of non-leading contributions to the BFKL Pomeron intercept by means of an effective theory describing the interactions of *reggeized gluons* with *elementary particles* (quarks and gluons). In the papers [9], such an effective action approach for inelastic high-energy scattering in QCD was suggested and developed. In the work by L.N. Lipatov of 1995, this approach was generalized to the processes with arbitrary number of produced particles separated into several groups by rapidity satisfying the multi-Regge kinematics conditions. As a result, the non-Abelian gauge invariant effective action for quasi-multi-Regge kinematics (QMRK) processes was derived [10]. This action allows to take into account arbitrary number of produced particles and contains the fields of two sorts: the *reggeized gluons* in the t -channel, and the ordinary gluons and quarks in the production channel.

The motivation of this work is necessity for developing a proper practical tool for explicit calculations of the next-to-leading corrections to Feynman inelastic amplitudes of peripheral processes. The first thing one has to do before doing any calculations is to derive the Feynman rules corresponding to an effective Lagrangian which is dealt with. In our case, such rules should prescribe the propagators of *reggeon* and ordinary particles as well as the effective reggeon-particle vertices. A number of such effective vertices was already calculated by L.N. Lipatov, V.S. Fadin *et al.* [11, 12], and A. Leonidov and D. Ostrovsky [13]. The string theory motivated approach to study the effective vertices was developed in Refs. [14].

In the present work, we obtain these and some other results within the unified framework of the gauge invariant effective action introduced in Ref. [10]. There is a hope that building and application of a set of such rules derived from the effective action can provide significant simplification of evaluation of differential cross sections related to creation of several particle clusters separated by rapidity gaps. We concentrate our attempts on presentation of the results in the form most convenient for use in numerical simulations for phenomenological applications.

The processes of such a kind can be investigated, *e.g.*, in experiments at RHIC and LHC. Another important branch of possible applications—calculation of peripheral amplitudes with several reggeized gluon states in the scattering channel—is out of scope of the present paper and will not be considered here.

The structure of the paper is following: In the Section II, we fix the notations and give an elementary “vocabulary” of terms and kinematics relations that are used in the work. In the Section III, several Reggeon-Particle vertices are derived systematically within the effective gauge invariant action approach and presented in an explicit analytical form. In the Section IV, we discuss the calculation of the cross section for the multi-jet production process in the QMRK using the effective vertices derived in this paper. In Conclusions, we summarize the results and propose possible applications of them in high energy phenomenology.

II. VOCABULARY

Let us give a “vocabulary” which is used throughout the present work. We consider the parton-parton collision at high energy in the center-of-mass system. The main contribution to the total cross section stems from the QMRK of final state particles (see Fig.1). In this regime, the final state particles compose several groups with arbitrary number of gluons, or quarks with fixed masses M_i , which are produced in the Regge kinematics with respect to each other:

$$P_A + P_B = Q_1 + Q_2 + \dots + Q_n ,$$

$$s = 2P_A P_B = 4E^2 \gg s_i = 2Q_i Q_{i+1} \gg |t_i| = |q_i^2| , i = 1, 2, \dots, n-1 ;$$

$$Q_i^2 = M_i^2 , Q_k = \sum p_j^{(k)} , k = 1, 2, \dots, n . \quad (1)$$

Also, we introduce the light-cone vectors

$$n^+ = \frac{P_B}{E} , n^- = \frac{P_A}{E} , n^+ n^- = 2 , (n^\pm)^2 = 0 \quad (2)$$

and thus the light-cone projections of momenta and derivatives read, respectively

$$k^\pm = (n_\mu)^\pm \cdot k^\mu , \partial_\pm = (n_\mu)^\pm \cdot \partial^\mu . \quad (3)$$

We imply also that the derivatives act on the particle $v(p)$ and reggeon $A(p)$ fields in the momentum representation as follows:

$$\partial_{\pm} v(p) = -ip_{\pm} v(p) , \quad \frac{1}{\partial_{\pm}} v(p) = \frac{i}{p_{\pm}} v(p) , \quad \partial_{\sigma}^2 A(q) = -q^2 A(q) . \quad (4)$$

Besides this, we define two transferred momentum 4-vectors:

$$q_1 = P_A - P_{A'} , \quad q_2 = P_B - P_{B'} \quad (5)$$

and their Sudakov decompositions

$$q_1 = q_{1\perp} + \frac{q_1^+}{2} n^- , \quad q_2 = q_{2\perp} + \frac{q_2^-}{2} n^+ , \quad q_1^- = q_2^+ = 0 . \quad (6)$$

The Sudakov variables for produced particles are:

$$p_i = \frac{p_i^+}{2} n^- + \frac{p_i^-}{2} n^+ + \mathbf{p}_{i\perp} . \quad (7)$$

In the fragmentation regions, one has

$$P_A + q_2 \rightarrow p_1 + p_2 + \dots + p_n : \quad P_A^+ = \sum_{i=1}^n p_i^+ , \quad |q_2^+| \ll p_i^+ , \quad (8)$$

$$P_B + q_1 \rightarrow p_1 + p_2 + \dots + p_n : \quad P_B^- = \sum_{i=1}^n p_i^- , \quad |q_1^-| \ll p_i^- . \quad (9)$$

In central region one has

$$q_1 + q_2 \rightarrow \sum_{i=1}^n p_i , \quad q_1^+ = \sum_{i=1}^n p_i^+ ; \quad q_2^- = \sum_{i=1}^n p_i^- . \quad (10)$$

To each reggeized gluon line (existing only in the scattering channel), one should attribute the sign (+) to its end attached to initial parton with the momentum P_A , and the sign (-) to the end attached to parton with the momentum P_B . Note, that the vertical lines at the Fig. 1 represent the reggeons, or particles, which are *off*-mass-shell. Initial, final and produced particles (presented by not vertical lines at the Fig. 1) are the *on*-mass-shell particles, which we will suggest, as a rule, to be massless. Let us emphasize that the presence of reggeon lines within any production block is forbidden in the QMRK due to the rapidity gap, Eq. (1).

The effective action approach can be formulated in terms of the physical particles (quarks and gluons) and the reggeized gluons. It is convenient to write down the effective action in the following form:

$$S = \int dx [\mathcal{L}_{QCD} + \mathcal{L}_{ind}] , \quad (11)$$

where the standard Yang-Mills part consists of the quark-gluon and gluon-gluon interactions

$$\mathcal{L}_{QCD} = g\bar{\psi}T^a\gamma^\mu\psi v_\mu^a - \frac{1}{4}(\partial_\mu v_\nu^a - \partial_\nu v_\mu^a)^2 + \frac{g}{2}(abc)(\partial_\mu v_\nu^a)v_\mu^b v_\nu^c - \frac{g^2}{4}(lbc)(lde)v_\mu^b v_\nu^c v_\mu^d v_\nu^e . \quad (12)$$

Here and in what follows we use the notation for the $SU(N)$ gauge group structure constants:

$$f^{abc} \equiv (abc) . \quad (13)$$

The induced part contains gluon-reggeon couplings:

$$\mathcal{L}_{ind}(v_{\pm}, A_{\pm}) = - \int dx \text{Tr} \left\{ \left[v_+ - gv_+ \frac{1}{\partial_+} v_+ + g^2 v_+ \frac{1}{\partial_+} v_+ \frac{1}{\partial_+} v_+ - \dots - A_+ \right] \cdot \partial_{\sigma}^2 A_- + [v_+, \partial_+, A_{\pm} \rightarrow v_-, \partial_-, A_{\mp}] \right\} , \quad (14)$$

with $v_{\pm} \equiv T^a (n^{\pm})^{\mu} v_{\mu}^a$ are the particle (ordinary gluon) fields, and $A_{\pm} \equiv T^a (n^{\pm})^{\mu} A_{\mu}^a$ —the reggeized gluon fields. Note (see Ref. [10]), that in the QMRK the momenta of reggeons are transverse: $-q_i^2 \approx \mathbf{q}_i^2$, and the following relations hold in the effective vertices:

$$\partial_- A_+ = \partial_+ A_- = 0 .$$

For the hermitian color generators T^a , we use

$$[T^a, T^b] = i(abc)T^c \quad , \quad \text{Tr}(T^a T^b) = \frac{1}{2}\delta^{ab} . \quad (15)$$

For the ordinary YM 3-gluon vertices we imply all the momenta to be *in-coming*. For the color factors associated with ordinary, or effective 3-gluon vertices, Eq. 13, we imply the clockwise sequence of color indices.

III. VERTICES

A. Standard QCD Feynman rules

The Yang-Mills interaction part of the effective action yields the standard QCD Feynman rules (see Fig. 2a-c):

$$3g\text{-vertex} : \quad g(abc) [(p_1 - p_2)_{\lambda} g_{\mu\nu} + (p_2 - p_3)_{\mu} g_{\nu\lambda} + (p_3 - p_1)_{\nu} g_{\lambda\mu}] \equiv g(abc)\gamma_{\mu\nu\lambda}(p_1, p_2, p_3) , \quad (16)$$

having the property

$$\gamma_{\mu\nu\lambda}(p_1, p_2, p_3) = \gamma_{\lambda\mu\nu}(p_3, p_1, p_2) = -\gamma_{\nu\mu\lambda}(p_2, p_1, p_3) = \dots , \quad (17)$$

$$4g\text{-vertex} : \quad ig^2[(abl)(cdl)(g^{\mu\sigma}g^{\nu\lambda} - g^{\mu\lambda}g^{\nu\sigma}) + (acl)(dbl)(g^{\mu\nu}g^{\lambda\sigma} - g^{\mu\sigma}g^{\lambda\nu}) + (adl)(bcl)(g^{\mu\lambda}g^{\sigma\nu} - g^{\mu\nu}g^{\sigma\lambda})] \equiv ig^2\gamma_{abcd}^{\mu\nu\lambda\sigma} , \quad \gamma_{abcd}^{\mu\nu\lambda\sigma} = \gamma_{bacd}^{\nu\mu\lambda\sigma} = \dots , \quad (18)$$

$$\text{gluon propagator:} \quad -i\delta^{ab} \frac{g_{\mu\nu}}{k^2} , \quad (19)$$

$$\text{quark-gluon vertex:} \quad ig\bar{u}(p_1)\gamma^{\mu}T^a u(p_2) , \quad (20)$$

$$\text{quark propagator:} \quad i\frac{\hat{p} + m}{p^2 + m^2} . \quad (21)$$

In addition, we specify the reggeized gluon propagator, Fig. 2d:

$$-\frac{i}{2k^2}\delta^{ab} [(n^+)^{\mu}(n^-)^{\nu} + (n^+)^{\nu}(n^-)^{\mu}] . \quad (22)$$

B. Lowest order induced vertices

Induced part of the action takes into account emission of initial particles in the fragmentation region. The simplest particle-reggeon (PR) vertex in the momentum space is defined as (see Fig. 3a)

$$i\langle 0 | \mathcal{L}_{ind}^{PR} | v_a^{\nu}(q) A_{\pm b} \rangle = V_{ab}^{\pm\nu}(q) , \quad \mathcal{L}_{ind}^{PR} = -\text{Tr}(v_+ \partial_{\sigma}^2 A_- + v_- \partial_{\sigma}^2 A_+) , \quad (23)$$

and is given by

$$V_{ab}^{\pm\nu}(q) = i\delta^{ab} q^2 (n^{\pm})^{\nu} . \quad (24)$$

One can easily check fulfillment of the gauge invariance condition for this vertex:

$$q_{2\nu} \cdot V_{ab}^{+\nu}(q_2) = 0 , \quad q_{1\nu} \cdot V_{ab}^{-\nu}(q_1) = 0 . \quad (25)$$

The induced vertices of the PPR type (vertices of the first rank) for *fragmentation* regions read (see Fig. 3b)

$$g\Delta_{abc}^{\nu\eta+}(P_A, P_{A'}, q_2) = \left\langle 0 \left| -ig\text{Tr} \left[v_+ \frac{1}{\partial_+} v_+ \partial_\sigma^2 A_- \right] \left| v_a^\nu(P_A) v_b^\eta(P_{A'}) A_{+c}(q_2) \right. \right\rangle = g(abc) \frac{q_2^2}{P_A^+} (n^+)^\nu (n^+)^\eta, \quad (26)$$

$$g\Delta_{cab}^{-\nu\eta}(q_1, P_{B'}, P_B) = \left\langle 0 \left| -ig\text{Tr} \left[v_- \frac{1}{\partial_-} v_- \partial_\sigma^2 A_+ \right] \left| v_a^\nu(P_B) v_b^\eta(P_{B'}) A_{-c}(q_1) \right. \right\rangle = -g(cba) \frac{q_1^2}{P_B^-} (n^-)^\nu (n^-)^\eta, \quad (27)$$

where we imply that

$$P_A^+ = P_{A'}^+, \quad P_B^- = P_{B'}^-; \quad q_1 = P_{B'} - P_B, \quad q_2 = P_{A'} - P_A.$$

The induced PPR vertices in the *central* region are

$$g\Delta_{cba}^{-\eta\nu}(q_1, k, q_2) = -g(cba) \frac{q_1^2}{q_2} (n^-)^\nu (n^-)^\eta, \quad (28)$$

—the “left” induced vertex (see Fig. 3c-left), and

$$g\Delta_{abc}^{\nu\eta+}(q_1, k, q_2) = g(abc) \frac{q_1^2}{q_1^+} (n^+)^\nu (n^+)^\eta, \quad (29)$$

—the “right” induced vertex (see Fig. 3c-right), where $k = q_1 + q_2$.

In the higher order calculations, it turns out to be more convenient to use the recurrent relations (see Appendix B) instead of direct calculation by means of the Eq. (14).

For the “left” induced vertex of the second rank (see Fig. 3d-left) we have

$$\begin{aligned} \Delta_{ca_1a_2d}^{-\nu_1\nu_2\eta}(q_1, p_1, p_2, q_2) = \\ \frac{(n^-)^{\nu_2}}{p_2^-} \left[(ma_2a_1)\Delta_{cmd}^{-\nu_1\eta}(q_1, p_1 + p_2, q_2) + (ma_2d)\Delta_{ca_1m}^{-\nu_1\eta}(q_1, p_1, q_2 - p_2) \right] = \\ -\frac{q_1^2}{p_2^-} \left[\frac{(ma_2a_1)(cmd)}{q_2^-} + \frac{(ma_2a_1)(cmd)}{p_1^-} \right] (n^-)^{\nu_1} (n^-)^{\nu_2} (n^-)^\eta, \quad q_2^- = p_1^- + p_2^-. \end{aligned} \quad (30)$$

For the “right” vertex (see Fig. 3d-right) we have

$$\begin{aligned} \Delta_{ca_1a_2d}^{\rho\nu_1\nu_2+}(q_1, p_1, p_2, q_2) = \\ \frac{(n^+)^{\nu_2}}{p_2^+} \left[(ma_2c)\Delta_{ma_1d}^{\rho\nu_1+}(q_1 - p_2, p_1, q_2) + (ma_2a_1)\Delta_{cmd}^{\rho\nu_1+}(q_1, p_1 + p_2, q_2) \right] = \\ \frac{q_2^2}{p_2^+} \left[\frac{(ma_2c)(ma_1d)}{p_1^+} + \frac{(ma_2a_1)(cmd)}{q_1^+} \right] (n^+)^{\nu_1} (n^+)^{\nu_2} (n^+)^\rho, \quad q_1^+ = p_1^+ + p_2^+. \end{aligned} \quad (31)$$

The induced vertices of next ranks will be specified below. One can verify the fulfillment of the Bose-symmetry requirements: expressions for Δ 's remain the same under simultaneous replacements of color and Lorentz indices and the momenta of any pair of particles. This fact is a consequence of conservation law and the Jacobi identity.

C. Effective PPR vertices

Knowledge of the induced and ordinary 3-vertices allows one to build the effective 3-vertices which obey the Bose- and gauge-symmetries. We distinguish four types of the PPR vertices. First group consists of the margin type vertices: $q_2 = -P_A + P_{A'}$, $q_1 = P_{B'} - P_B$.

- “Left” margin type (see Fig. 4a):

$$\gamma_{\parallel abc}^{\nu\nu'+} (P_A, a; P_{A'}, b; q_2, c) = g(abc) \Gamma^{\nu\nu'+} (P_A, q_2) ,$$

$$\Gamma^{\nu\nu'+} (P_A, q_2) = 2P_A^+ g^{\nu\nu'} + (n^+)^{\nu} (-2P_A + P_{A'})^{\nu'} + (n^+)^{\nu'} (-2P_{A'} + P_A)^{\nu} - \frac{q_2^2}{P_A^+} (n^+)^{\nu} (n^+)^{\nu'} . \quad (32)$$

One can check that the condition of gauge invariance is explicitly satisfied:

$$\Gamma^{\nu\nu'+} (P_A, q_2) \cdot (P_{A'})_{\nu'} = P_A^{\nu} P_A^+ - P_A^2 (n^+)^{\nu} \quad (33)$$

$$\Gamma^{\nu\nu'+} (P_A, q_2) \cdot (P_A)_{\nu} = P_{A'}^{\nu'} P_A^+ - P_{A'}^2 (n^+)^{\nu'} . \quad (34)$$

For *on*-mass-shell particle A : $P_A^2 = 0$ with the gauge condition $(e(P_A) \cdot P_A) = 0$ we have

$$\Gamma^{\nu\nu'+} (P_A, q_2) \cdot (P_{A'})_{\nu'} \cdot e_{\nu} (P_A) = 0 . \quad (35)$$

- “Right” margin type (see Fig. 4b):

$$\gamma_{\parallel}^{\nu\nu'-} (P_B, a; P_{B'}, b; q_1, c) = -g(bac) \Gamma^{\nu\nu'-} (q_1, P_B) ,$$

$$\Gamma^{\nu\nu'-} (q_1, P_B) = 2P_B^- g^{\nu\nu'} - (n^-)^{\nu'} (2P_{B'} - P_B)^{\nu} - (n^-)^{\nu} (2P_B - P_{B'})^{\nu'} - \frac{q_1^2}{P_B^-} (n^-)^{\nu} (n^-)^{\nu'} . \quad (36)$$

In this case, the gauge-invariance tests read

$$\Gamma^{\nu\nu'-} (q_1, P_B) \cdot (P_{B'})_{\nu'} = P_B^{\nu} P_B^- - P_B^2 (n^-)^{\nu} , \quad (37)$$

$$\Gamma^{\nu\nu'-} (q_1, P_B) \cdot (P_B)_{\nu} = P_{B'}^{\nu'} P_B^- - P_{B'}^2 (n^-)^{\nu'} . \quad (38)$$

The second group includes the effective vertices of the *central* type where $k = q_1 + q_2$, $q_{1,2}^2 \neq 0$:

- “Left” central type (see Fig. 4c):

$$\gamma_{\perp abc}^{\nu\nu'+} (q_1, a; k, b; q_2, c) = g(abc) \Gamma^{\nu\nu'+} (q_1, q_2) ,$$

$$\Gamma^{\nu\nu'+} (q_1, q_2) = 2q_1^+ g^{\nu\nu'} - (n^+)^{\nu} (q_1 - q_2)^{\nu'} - (n^+)^{\nu'} (q_1 + 2q_2)^{\nu} - \frac{q_2^2}{q_1^+} (n^+)^{\nu} (n^+)^{\nu'} . \quad (39)$$

The corresponding Ward identities read:

$$\Gamma^{\nu\nu'+} (q_1, q_2) \cdot k_{\nu'} = q_1^+ q_1^{\nu} - q_1^2 (n^+)^{\nu} , \quad \Gamma^{\nu\nu'+} (q_1, q_2) \cdot (q_1)_{\nu} = q_1^+ k^{\nu'} - k^2 (n^+)^{\nu'} . \quad (40)$$

- “Right” central type (see Fig. 4d):

$$\gamma_{\perp abc}^{\nu\nu'-} (q_1, a; k, b; q_2, c) = -g(abc) \Gamma^{\nu\nu'-} (q_1, q_2) ,$$

$$\Gamma^{\nu\nu'-} (q_1, q_2) = 2q_2^- g^{\nu\nu'} + (n^-)^{\nu} (q_1 - q_2)^{\nu'} + (n^-)^{\nu'} (-q_2 - 2q_1)^{\nu} - \frac{q_1^2}{q_2^-} (n^-)^{\nu} (n^-)^{\nu'} , \quad (41)$$

for which one has

$$\Gamma^{\nu\nu'-} (q_1, q_2) \cdot k_{\nu'} = q_2^- q_2^{\nu} - (n^-)^{\nu} q_2^2 , \quad \Gamma^{\nu\nu'-} (q_1, q_2) \cdot (q_2)_{\nu} = q_2^- k^{\nu'} - k^2 (n^-)^{\nu'} . \quad (42)$$

D. Effective PRR vertex

Production of a single gluon with momentum $k_\mu = (q_1 + q_2)_\mu$ and color index b in the “two reggeons collision” in color-momentum states, respectively, $(q_1, a; k, b; q_2, c)$, is described by the PRR vertex (see Fig. 4e)

$$\Gamma^{-\mu+}(q_1, a; k, b; q_2, c) = g(abc) C^\mu(q_1, q_2) ,$$

$$(abc)C^\mu(q_1, q_2) = (abc)\gamma^{\nu\mu\eta}(q_1, -k, q_2)(n^-)_\nu(n^+)_\eta + \Delta_{cba}^{-\mu\eta}(q_1, k, q_2)(n^+)_\eta - \Delta_{abc}^{\eta\mu+}(q_1, k, q_2)(n^-)_\eta . \quad (43)$$

As a result we have

$$C^\mu(q_1, q_2) = 2 \left[(n^-)^\mu \left(q_1^+ + \frac{q_1^2}{q_2} \right) - (n^+)^\mu \left(q_2^- + \frac{q_2^2}{q_1^+} \right) + (q_2 - q_1)^\mu \right] . \quad (44)$$

The 4-vector C^μ obeys the gauge condition $k_\mu \cdot C^\mu(q_1, q_2) = 0$.

E. Effective $RRPP$ vertex

We consider first the case when pair of gluons in color-momenta states $(p_1, \nu_1, a_1; p_2, \nu_2, a_2)$ are created in collision of two reggeons with color-momenta states $(q_1, c; q_2, d)$ with the momentum conservation relation $q_1 + q_2 = p_1 + p_2$. It can be build in terms of the effective 3-vertices given above (see Fig. 4) It has the form

$$\begin{aligned} & \frac{1}{ig^2} \Gamma_{ca_1a_2d}^{-\nu_1\nu_2+}(q_1; p_1, p_2; q_2) = \\ & = \frac{T_1}{p_{12}^2} C^\eta(q_1, q_2) \gamma^{\nu_1\nu_2\eta}(-p_1, -p_2, p_{12}) + \frac{T_3}{(p_2 - q_2)^2} \Gamma^{\eta\nu_1-}(q_1, p_1 - q_1) \Gamma^{\eta\nu_2+}(p_2 - q_2, q_2) - \\ & \quad \frac{T_2}{(p_1 - q_2)^2} \Gamma^{\eta\nu_2-}(q_1, p_2 - q_1) \Gamma^{\eta\nu_1+}(p_1 - q_2, q_2) - \\ & T_1 [(n^-)^{\nu_1} (n^+)^{\nu_2} - (n^-)^{\nu_2} (n^+)^{\nu_1}] - T_2 [2g^{\nu_1\nu_2} - (n^-)^{\nu_1} (n^+)^{\nu_2}] - T_3 [(n^-)^{\nu_2} (n^+)^{\nu_1} - 2g^{\nu_1\nu_2}] + \\ & \quad \Delta_{ca_1a_2d}^{\rho\nu_1\nu_2+}(q_1, p_1, p_2, q_2)(n^-)_\rho + \Delta_{ca_1a_2d}^{-\nu_1\nu_2\eta}(q_1, p_1, p_2, q_2)(n^+)_\eta , \end{aligned} \quad (45)$$

where

$$T_1 = (a_1a_2r)(cdr) , T_2 = (a_2cr)(a_1dr) , T_3 = (ca_1r)(a_2dr) , T_1 + T_2 + T_3 = 0 , \quad (46)$$

and the induced vertices, Fig. 3e:

$$\Delta_{ca_1a_2d}^{\rho\nu_1\nu_2+}(q_1, p_1, p_2, q_2)(n^-)_\rho = -2q_2^2 (n^+)^{\nu_1} (n^+)^{\nu_2} \left(\frac{T_3}{p_2^+ q_1^+} - \frac{T_2}{p_1^+ q_1^+} \right) , \quad (47)$$

$$\Delta_{ca_1a_2d}^{-\nu_1\nu_2\eta}(q_1, p_1, p_2, q_2)(n^+)_\eta = -2q_1^2 (n^-)^{\nu_1} (n^-)^{\nu_2} \left(\frac{T_3}{p_1^- q_2^-} - \frac{T_2}{p_2^- q_2^-} \right) . \quad (48)$$

One can verify the fulfillment of the gauge- and Bose-symmetries requirements:

$$\Gamma_{ca_1a_2d}^{-\nu_1\nu_2+}(q_1; p_1, p_2; q_2) p_{1\nu_1} = 0 , \Gamma_{ca_1a_2d}^{-\nu_1\nu_2+}(q_1; p_1, p_2; q_2) = \Gamma_{ca_2a_1d}^{-\nu_2\nu_1+}(q_1; p_2, p_1; q_2) . \quad (49)$$

F. Effective $PPPR$ vertices

Let us consider now the margin $PPPR$ vertices. The effective $PPPR$ vertex can be constructed in terms of combination of previously calculated effective vertices, and ordinary 3-vertices (see Figs. 6, 7).

For the vertex describing the A -particle fragmentation region to two gluons and a reggeon $P_A + R(q_2) \rightarrow g_1(p_1) + g_2(p_2)$ (see Fig. 6), one has

$$\begin{aligned} & \frac{1}{ig^2} \Gamma_{ca_1a_2d}^{\nu_0\nu_1\nu_2+} (P_A, p_1, p_2, q_2) = \\ & = \frac{T_1}{p_{12}^2} \gamma^{\sigma\nu_1\nu_2} (p_{12}, -p_1, -p_2) \Gamma^{\nu_0\sigma+} (P_A, q_2) + \frac{T_3}{(p_2 - q_2)^2} \gamma^{\nu_0\nu_1\sigma} (P_A, -p_1, p_1 - P_A) \Gamma^{\sigma\nu_2+} (p_2 - q_2, q_2) + \\ & \frac{T_2}{(p_1 - q_2)^2} \gamma^{\nu_0\nu_2\sigma} (P_A, -p_2, p_2 - P_A) \Gamma^{\sigma\nu_1+} (p_1 - q_2, q_2) + T_3 [g^{\nu_1\nu_2} (n^+)^{\nu_0} - (n^+)^{\nu_1} g^{\nu_0\nu_2}] + \\ & T_2 [g^{\nu_0\nu_1} (n^+)^{\nu_2} - g^{\nu_1\nu_2} (n^+)^{\nu_0}] + T_1 [(n^+)^{\nu_1} g^{\nu_0\nu_2} - (n^+)^{\nu_2} g^{\nu_0\nu_1}] + \Delta_{ca_1a_2d}^{\nu_0\nu_1\nu_2+} (P_A, p_1, p_2, q_2) , \end{aligned} \quad (50)$$

with the same definition for T_i 's as for the case $RRPP$ effective vertex, Eq. (46), and the conservation law $P_A + q_2 = p_1 + p_2$. When checking the gauge invariance (convoluting with $(p_1)_{\nu_1}$) we use the expression for the induced vertex (see Fig. 3d-left)

$$\Delta_{ca_1a_2d}^{\nu_0\nu_1\nu_2+} (P_A, p_1, p_2, q_2) = \frac{q_2^2}{P_A^+} \left[2 \frac{T_2}{p_1^+} - \frac{T_3}{p_2^+} \right] (n^+)^{\nu_0} (n^+)^{\nu_1} (n^+)^{\nu_2} . \quad (51)$$

One can verify the fulfillment of the gauge condition:

$$\Gamma_{ca_1a_2d}^{\nu_0\nu_1\nu_2+} (P_A, p_1, p_2, q_2) \cdot (p_1)_{\nu_1} = 0 , \quad (52)$$

as well as the Bose-symmetry condition:

$$\Gamma_{ca_1a_2d}^{\nu_0\nu_1\nu_2+} (P_A, p_1, p_2, q_2) = \Gamma_{ca_2a_1d}^{\nu_0\nu_2\nu_1+} (P_A, p_2, p_1, q_2) = \dots . \quad (53)$$

Similarly, we find for the ‘‘right’’ effective *margin* vertex, Fig. 7:

$$\begin{aligned} & \frac{1}{ig^2} \Gamma_{ca_1a_2d}^{-\nu_1\nu_2\nu_0} (q_1, p_1, p_2, P_B) = \\ & - \frac{T_1}{p_{12}^2} \gamma^{\sigma\nu_1\nu_2} (p_{12}, -p_1, -p_2) \Gamma^{\nu_0\sigma-} (q_1, p_{12} - q_1) + \frac{T_3}{(p_1 - q_1)^2} \gamma^{\sigma\nu_2\nu_0} (p_2 - P_B, -p_2, P_B) \Gamma^{\sigma\nu_1-} (q_1, p_1 - q_1) - \\ & \frac{T_2}{(p_2 - q_1)^2} \gamma^{\sigma\nu_1\nu_0} (p_1 - P_B, -p_1, P_B) \Gamma^{\sigma\nu_2-} (q_1, p_2 - q_1) + T_1 [(n^-)^{\nu_2} g^{\nu_0\nu_1} - (n^-)^{\nu_1} g^{\nu_0\nu_2}] + \\ & T_3 [g^{\nu_1\nu_2} (n^-)^{\nu_0} - (n^-)^{\nu_2} g^{\nu_0\nu_1}] + T_2 [(n^-)^{\nu_1} g^{\nu_0\nu_2} - (n^-)^{\nu_0} g^{\nu_1\nu_2}] + \Delta_{ca_1a_2d}^{-\nu_1\nu_2\nu_0} (q_1, p_1, p_2, P_B) , \end{aligned} \quad (54)$$

with the same notations for T_i 's as for ‘‘left’’ margin vertex and the $RRPP$ vertex, Eq. (46), conservation law $q_1 + P_B = p_1 + p_2$, and the induced vertex, Fig. 3d-right:

$$\Delta_{ca_1a_2d}^{-\nu_1\nu_2\nu_0} (q_1, p_1, p_2, P_B) = \frac{q_1^2}{P_B^-} \left[\frac{T_2}{p_2^-} - \frac{T_3}{p_1^-} \right] (n^-)^{\nu_0} (n^-)^{\nu_1} (n^-)^{\nu_2} . \quad (55)$$

Again, the gauge condition is fulfilled:

$$\Gamma_{da_1a_2c}^{-\nu_1\nu_2\nu_0} (q_1, p_1, p_2, P_B) \cdot (p_1)_{\nu_1} = 0 , \quad (56)$$

as well as the Bose-symmetry.

G. Effective $RRPPP$, and $RPPPP$ vertices

- Consider first the $RRPPP$ vertex $V^{+\nu_1\nu_2\nu_3-}(q_1, p_1, p_2, p_3, q_2)$. It can be constructed by means of combinations of the already known effective vertices given above, Eqs. (16, 18, 19, 24, 39, 41). The result is graphically presented at the Fig. 8. Each of these diagrams presents, indeed, a set of diagrams related to each other by any possible permutations of the produced particles. Using the rules given in Appendix A one can write down the analytical expression summing up all these contributions:

$$\begin{aligned}
& \frac{1}{g^3} \Gamma_{d123e}^{-\nu_1\nu_2\nu_3+}(q_1, p_1, p_2, p_3, q_2) = \frac{(edr)}{k^2} C_\sigma(q_1, q_2) \cdot A_{a_1 a_2 a_3 r}^{\nu_1\nu_2\nu_3\sigma} + \\
& \left[(mdr)(r13)(em2) \frac{1}{p_{13}^2(p_2 - q_2)^2} \Gamma^{\sigma\eta-}(q_1, p_{13} - q_1) \Gamma^{\sigma\nu_2+}(p_2 - q_2, q_2) \gamma^{\nu_1\nu_3\eta}(-p_1, -p_3, p_{13}) + 2 \text{ perm.} \right] + \\
& \left[(md3)(r12)(emr) \frac{1}{p_{12}^2(p_3 - q_1)^2} \Gamma^{\sigma\nu_3-}(q_1, p_3 - q_1) \Gamma^{\sigma\eta+}(p_{12} - q_2, q_2) \gamma^{\nu_1\nu_2\eta}(-p_1, -p_2, p_{12}) + 2 \text{ perm.} \right] + \\
& \left[(md1)(rm2)(er3) \frac{1}{(q_1 - p_1)^2(p_3 - q_2)^2} \Gamma^{\sigma\nu_1-}(q_1, p_1 - q_1) \Gamma^{\eta\nu_3+}(p_3 - q_2, q_2) \gamma^{\sigma\nu_2\eta}(q_1 - p_1, -p_2, q_2 - p_3) + 5 \text{ perm.} \right] + \\
& \left[(er3) \frac{1}{(p_3 - q_2)^2} \Gamma^{\sigma\nu_3+}(p_3 - q_2, q_2) (\Delta + \gamma)_{d12r}^{-\nu_1\nu_2\sigma}(q_1, p_1, p_2, q_2 - p_3) + 2 \text{ perm.} \right] - \\
& \left[(rd3) \frac{1}{(p_3 - q_1)^2} \Gamma^{\sigma\nu_3-}(q_1, p_3 - q_1) (\Delta + \gamma)_{r12e}^{\sigma\nu_1\nu_2+}(q_1 - p_3, p_1, p_2, q_2) + 2 \text{ perm.} \right] + \\
& \left[(r23) \frac{1}{p_{23}^2} \gamma^{\nu_2\nu_3\sigma}(-p_2 - p_3, p_{23}) (\Delta_{dr1e}^{-\sigma\nu_1\eta} \cdot (n^+)_{\eta} + \gamma_{dr1e}^{-\sigma\nu_1+} + \Delta_{dr1e}^{\rho\sigma\nu_1+} \cdot (n^-)_{\rho}) (q_1, p_{23}, p_1, q_2) + 2 \text{ perm.} \right] + \\
& (\Delta_{d123e}^{-\nu_1\nu_2\nu_3\rho} \cdot (n^+)_{\rho} + \Delta_{d123e}^{\rho\nu_1\nu_2\nu_3+} \cdot (n^-)_{\rho}) (q_1, p_1, p_2, p_3, q_2) , \tag{57}
\end{aligned}$$

where we use the shorthand notations

$$(123) \equiv (a_1 a_2 a_3) , \quad p_{12} = p_1 + p_2 , \quad k = p_1 + p_2 + p_3 . \tag{58}$$

For the induced terms of the rank-2 entering $RRPPP$ we have (see Fig. 3g):

$$\Delta_{d12r}^{-\nu_1\nu_2\sigma}(q_1, p_1, p_2, q_2 - p_3) = -\frac{q_1^2}{p_1} (n^-)^{\nu_1} (n^-)^{\nu_2} (n^-)^{\sigma} \left[\frac{(1mr)(2dr)}{p_2^-} + \frac{(mdr)(12r)}{p_{12}^-} \right] , \tag{59}$$

$$\Delta_{dr1e}^{-\sigma\nu_1\eta}(q_1, p_{23}, p_1, q_2) = -\frac{q_1^2}{p_1} (n^-)^{\nu_1} (n^-)^{\eta} (n^-)^{\sigma} \left[\frac{(1er)(dmr)}{p_{23}^-} + \frac{(edr)(1mr)}{q_2^-} \right] , \tag{60}$$

$$\Delta_{r12e}^{\sigma\nu_1\nu_2+}(q_1 - p_3, p_1, p_2, q_2) = \frac{q_2^2}{p_1^+} (n^+)^{\nu_1} (n^+)^{\nu_2} (n^+)^{\sigma} \left[\frac{(12r)(emr)}{p_{12}^+} + \frac{(2er)(1mr)}{p_2^+} \right] , \tag{61}$$

$$\Delta_{dr1e}^{\rho\sigma\nu_1+}(q_1, p_{23}, p_1, q_2) = \frac{q_2^2}{p_1^+} (n^+)^{\nu_1} (n^+)^{\rho} (n^-)^{\sigma} \left[\frac{(d1r)(emr)}{p_{23}^+} + \frac{(edr)(1mr)}{q_1^+} \right] , \tag{62}$$

with conservation law

$$q_1^+ = p_1^+ + p_2^+ + p_3^+ , \quad q_2^- = p_1^- + p_2^- + p_3^- .$$

- For the “left” *margin* effective vertex of the rank-3 we have:

$$\begin{aligned}
\frac{1}{g^3} \Gamma_{d123e}^{\rho\nu_1\nu_2\nu_3+}(P_A, p_1, p_2, p_3, q_2) &= \frac{(edr)}{k^2} \Gamma^{\rho\sigma+}(P_A, q_2) \cdot A_{r123}^{\sigma\nu_1\nu_2\nu_3} - \left[(md1)(rm2)(er3) \frac{1}{(P_A - p_1)^2(p_3 - q_2)^2} \right. \\
&\quad \left. \Gamma^{\eta\nu_3+}(p_3 - q_2, q_2) \gamma^{\sigma\nu_2\eta}(P_A - p_1, -p_2, q_2 - p_3) \gamma^{\rho\nu_1\sigma}(P_A, -p_1, p_1 - P_A) + 5 \text{ perm.} \right] - \\
&\quad \left[(rdm)(m12)(er3) \frac{1}{p_{12}^2(p_3 - q_2)^2} \Gamma^{\eta\nu_3+}(p_3 - q_2, q_2) \gamma^{\rho\sigma\eta}(P_A, -p_{12}, q_2 - p_3) \gamma^{\sigma\nu_1\nu_2}(p_{12}, -p_1, -p_2) + 2 \text{ perm.} \right] + \\
&\quad \left[(md1) \frac{1}{(p_1 - P_A)^2} \gamma^{\rho\nu_1\sigma}(P_A, -p_1, p_1 - P_A) \left[-\frac{1}{p_{23}^2} \Gamma^{\sigma\eta+}(p_{23} - q_2, q_2) \gamma^{\nu_2\nu_3\eta}(-p_2, -p_3, p_{23})(emr)(r23) + \right. \right. \\
&\quad \left. \left. + (\Delta + \gamma)_{m23e}^{\sigma\nu_2\nu_3+}(P_A - p_1, p_2, p_3, q_2) \right] + 2 \text{ perm.} \right] + \left[(er1) \frac{1}{(p_1 - q_2)^2} \Gamma^{\sigma\nu_1+}(p_1 - q_2, q_2) \gamma_{d23r}^{\rho\nu_2\nu_3\sigma} + 2 \text{ perm.} \right] + \\
&\quad \left[\frac{(r23)}{p_{23}^2} \gamma^{\nu_2\nu_3\eta}(-p_2, -p_3, p_{23}) (\Delta + \gamma)_{dr1e}^{\rho\eta\nu_1+}(P_A, p_{23}, p_1, q_2) + 2 \text{ hboxperm.} \right] - \Delta_{d123e}^{\rho\nu_1\nu_2\nu_3+}(P_A, p_1, p_2, p_3, q_2), \quad (63)
\end{aligned}$$

where the “left” *margin* induced vertex, Fig. 3d-left, reads

$$\Delta_{m23e}^{\sigma\nu_2\nu_3+}(P_A - p_1, p_2, p_3, q_2) = \frac{q_2^2}{p_{23}^+} (n^+)^\sigma (n^+)^{\nu_2} (n^+)^{\nu_3} \left(\frac{(3em)(erm)}{p_3^+} - \frac{(e2m)(3rm)}{p_2^+} \right), \quad (64)$$

and

$$\Delta_{dr1e}^{\rho\eta\nu_1+}(P_A, p_{23}, p_1, q_2) = \frac{q_2^2}{p_1^+} (n^+)^\rho (n^+)^{\nu_1} (n^+)^\eta \left(-\frac{(emr)(1dr)}{p_{23}^+} - \frac{(m1r)(edr)}{P_A^+} \right), \quad (65)$$

and the conservation law $P_A^+ = p_1^+ + p_2^+ + p_3^+$ is implied.

- The “right” *margin* effective vertex is

$$\begin{aligned}
\frac{1}{g^3} \Gamma_{e123d}^{-\nu_1\nu_2\nu_3\rho}(q_1, p_1, p_2, p_3, P_B) &= -\frac{(der)}{k^2} \Gamma^{\rho\sigma-}(q_1, P_B) \cdot A_{r123}^{\sigma\nu_1\nu_2\nu_3} + \left[(me1)(rm2)(dr3) \frac{1}{(P_B - p_3)^2(p_1 - q_1)^2} \right. \\
&\quad \left. \Gamma^{\sigma\nu_1-}(q_1, p_1 - q_1) \gamma^{\eta\sigma\nu_2}(P_B - p_3, q_1 - p_1, -p_2) \gamma^{\rho\eta\nu_3}(P_B, p_3 - P_B, -p_3) + 5 \text{ perm.} \right] + \\
&\quad \left[(drm)(m12)(re3) \frac{1}{p_{12}^2(p_3 - q_1)^2} \Gamma^{\sigma\nu_3-}(q_1, p_3 - q_1) \gamma^{\rho\sigma\eta}(P_B, p_{12} - P_B, -p_{12}) \gamma^{\eta\nu_1\nu_2}(p_{12}, -p_1, -p_2) + 2 \text{ perm.} \right] + \\
&\quad \left[(dr1) \frac{1}{(p_1 - P_B)^2} \gamma^{\rho\eta\nu_1}(P_B, p_1 - P_B, -p_1) \left[\frac{(rem)(m23)}{p_{23}^2} \Gamma^{\eta\sigma-}(q_1, p_{23} - q_1) \gamma^{\sigma\nu_2\nu_3}(p_{23}, -p_2, -p_3) + \right. \right. \\
&\quad \left. \left. (\Delta + \gamma)_{e23r}^{-\nu_2\nu_3\eta}(q_1, p_2, p_3, P_B - p_1) \right] + 2 \text{ perm.} \right] - \\
&\quad \left[(me1) \frac{1}{(p_1 - q_1)^2} \Gamma^{\sigma\nu_1-}(q_1, p_1 - q_1) \gamma_{m23d}^{\sigma\nu_2\nu_3\rho} + 2 \text{ perm.} \right] + \\
&\quad \left[\frac{(m23)}{p_{23}^2} \gamma^{\sigma\nu_2\nu_3}(p_{23}, -p_2, -p_3) (\Delta + \gamma)_{em1d}^{-\sigma\nu_1\rho}(q_1, p_{23}, p_1, P_B) + 2 \text{ perm.} \right] - \Delta_{e123d}^{-\nu_1\nu_2\nu_3\rho}(q_1, p_1, p_2, p_3, P_B), \quad (66)
\end{aligned}$$

with the induced vertex, Fig. 3d-right:

$$\Delta_{e23r}^{-\nu_2\nu_3\eta}(q_1, p_2, p_3, P_B - p_1) = \frac{q_1^2}{p_{23}^-} (n^-)^{\nu_2} (n^-)^{\nu_3} (n^-)^\eta \left[\frac{(3em)(2rm)}{p_3^-} - \frac{(e2m)(3rm)}{p_2^-} \right], \quad (67)$$

and

$$\Delta_{em1d}^{-\sigma\nu_1\rho}(q_1, p_{23}, p_1, P_B) = \frac{q_1^2}{p_1^-} (n^-)^{\nu_1} (n^-)^\rho (n^-)^\sigma \left[\frac{(edr)(1mr)}{P_B^-} - \frac{(d1r)(emr)}{p_{23}^-} \right], \quad (68)$$

and the conservation law $P_B^- = p_1^- + p_2^- + p_3^-$.

Here by term “perm.” we imply all the terms obtained from the explicitly written the one which can be obtained by simultaneous permutations of the momenta, color and Lorentz indices. Like in the previous cases, the gauge invariance and Bose-symmetry properties are fulfilled explicitly. Some useful relations which can be used are presented in Appendix B.

The “left” induced vertex of the rank-3 has a form

$$\Delta_{d123e}^{\rho\nu_1\nu_2\nu_3+}(q_1, p_1, p_2, p_3, q_2) = q_2^2 (n^+)^\rho (n^+)^{\nu_1} (n^+)^{\nu_2} (n^+)^{\nu_3} \frac{D^+(q_1, d; p_1, a_1; p_2, a_2; p_3, a_3; q_2, e)}{p_1^+}, \quad (69)$$

where

$$D^+(q_1, d; p_1, a_1; p_2, a_2; p_3, a_3; q_2, e) = \frac{1}{p_{23}^+} \left[\frac{\alpha_1}{p_2^+} - \frac{\alpha_2}{p_3^+} \right] + \frac{1}{p_{12}^+} \left[\frac{\alpha_3}{q_1^+} + \frac{\alpha_4}{p_3^+} \right] + \frac{1}{p_{13}^+} \left[\frac{\alpha_5}{q_1^+} + \frac{\alpha_6}{p_2^+} \right], \quad (70)$$

and

$$\begin{aligned} \alpha_1 &= (md1)(e2r)(3mr); & \alpha_2 &= (md1)(3er)(2mr); & \alpha_3 &= (m12)(der)(3mr); \\ \alpha_4 &= (m12)(e3r)(dmr); & \alpha_5 &= (m13)(der)(2mr); & \alpha_6 &= (m13)(e2r)(dmr). \end{aligned} \quad (71)$$

Let us demonstrate the Bose-symmetry of this expression:

$$\begin{aligned} D^+(q_1, d; p_1, a_1; p_2, a_2; p_3, a_3; q_2, e) &= D^+(q_1, d; p_1, a_1; p_3, a_3; p_2, a_2; q_2, e); \\ \frac{D^+(q_1, d; p_1, a_1; p_2, a_2; p_3, a_3; q_2, e)}{p_1^+} &= \frac{D^+(q_1, d; p_2, a_2; p_1, a_1; p_3, a_3; q_2, e)}{p_2^+}. \end{aligned} \quad (72)$$

In fact, the first relation is obvious by construction. To show the validity of the second one, let us note that the expression

$$\frac{1}{p_2^+} \left[\frac{1}{p_{13}^+} \left(\frac{\beta_1}{p_1^+} - \frac{\beta_2}{p_3^+} \right) + \frac{1}{p_{12}^+} \left(\frac{\beta_3}{q_1^+} + \frac{\beta_4}{p_3^+} \right) + \frac{1}{p_{23}^+} \left(\frac{\beta_5}{q_1^+} + \frac{\beta_6}{p_1^+} \right) \right],$$

where

$$\begin{aligned} \beta_1 &= (md2)(e1r)(3mr); & \beta_2 &= (md2)(3er)(1mr); & \beta_3 &= (m21)(der)(3mr); \\ \beta_4 &= (m21)(e3r)(dmr); & \beta_5 &= (m23)(der)(1mr); & \beta_6 &= (m23)(e1r)(dmr). \end{aligned} \quad (73)$$

which is indeed the r.h.s. of the second equation, can be rearranged using the conservation law $q_1^+ = p_1^+ + p_2^+ + p_3^+$ and the relations

$$\beta_1 = -\alpha_2 + \alpha_4 + \alpha_5 + \alpha_6; \quad \beta_2 = \alpha_2 - \alpha_4; \quad \beta_3 = -\alpha_3; \quad \beta_4 = -\alpha_4; \quad \beta_5 = -\alpha_3 + \alpha_5; \quad \beta_6 = \alpha_1 + \alpha_2 + \alpha_3 - \alpha_5$$

giving the l.h.s. of the Eq. (72).

For the “right” induced vertex of the rank-3 (Fig. 3g-right) we have

$$\Delta_{da_1a_2a_3e}^{-\nu_1\nu_2\nu_3\rho}(q_1, p_1, p_2, p_3, q_2) = q_1^2 (n^-)^{\nu_1} (n^-)^{\nu_2} (n^-)^{\nu_3} (n^-)^\rho \frac{D^-(q_1, d; p_1, a_1; p_2, a_2; p_3, a_3; q_2, e)}{p_1^-}, \quad (74)$$

where

$$D^-(q_1, d; p_1, a_1; p_2, a_2; p_3, a_3; q_2, e) = \frac{1}{p_{23}^-} \left(\frac{\gamma_1}{p_3^-} - \frac{\gamma_2}{p_2^-} \right) - \frac{1}{p_{12}^-} \left(\frac{\gamma_3}{q_2^-} + \frac{\gamma_4}{p_3^-} \right) - \frac{1}{p_{13}^-} \left(\frac{\gamma_5}{q_2^-} + \frac{\gamma_6}{p_2^-} \right), \quad (75)$$

and

$$\begin{aligned} \gamma_1 &= (m1e)(3dr)(2mr) ; & \gamma_2 &= (m1e)(d2r)(3mr) ; & \gamma_3 &= (m12)(der)(3mr) ; \\ \gamma_4 &= (m12)(3dr)(emr) ; & \gamma_5 &= (m13)(der)(2mr) ; & \gamma_6 &= (m13)(2dr)(emr) . \end{aligned} \quad (76)$$

The Bose-symmetry can be proven similarly to the case of the ‘‘right’’ induced vertex of the rank-4, if one takes into account the relation

$$\Delta_{ea_1a_2a_3d}^{-\nu_1\nu_2\nu_3\rho}(q_1, p_1, p_2, p_3, q_2) = \Delta_{da_1a_2a_3e}^{\rho\nu_1\nu_2\nu_3+}(q_1, p_1, p_2, p_3, q_2) \Big|_{p_i^+ \rightarrow p_i^- ; d \rightarrow e ; e \rightarrow d; q_1^+ \rightarrow q_2^-} . \quad (77)$$

Besides this, let us note that the *margin* induced vertices of the rank-3 are connected with the *central* ones:

$$\Delta_{da_1a_2a_3e}^{-\nu_1\nu_2\nu_3\rho}(q_1, p_1, p_2, p_3, P_B) = \Delta_{ea_1a_2a_3d}^{-\nu_1\nu_2\nu_3\rho}(q_1, p_1, p_2, p_3, q_2) \Big|_{q_2 \rightarrow P_B; d \rightarrow e; e \rightarrow d} , \quad (78)$$

$$\Delta_{ea_1a_2a_3d}^{\rho\nu_1\nu_2\nu_3+}(P_A, p_1, p_2, p_3, q_2) = \Delta_{ea_1a_2a_3d}^{\rho\nu_1\nu_2\nu_3+}(q_1, p_1, p_2, p_3, q_2) \Big|_{q_1 \rightarrow P_A} . \quad (79)$$

The effective 4-gluon vertex A reads

$$\begin{aligned} A_{a_1a_2a_3r}^{\nu_1\nu_2\nu_3\sigma} &= \tau_1 [g_{\nu_1\sigma}g_{\nu_2\nu_3} - g_{\nu_1\nu_3}g_{\nu_2\sigma}] + \tau_2 [g_{\nu_1\nu_2}g_{\nu_3\sigma} - g_{\nu_1\sigma}g_{\nu_2\nu_3}] + \\ &\tau_3 [g_{\nu_1\nu_3}g_{\nu_2\sigma} - g_{\nu_1\nu_2}g_{\nu_3\sigma}] + \frac{\tau_3}{p_{23}^2} \gamma_{\sigma\nu_1\rho}(k, -p_1, -p_2 - p_3) \gamma_{\rho\nu_2\nu_3}(p_2 + p_3, -p_2, -p_3) + \\ &\frac{\tau_2}{p_{13}^2} \gamma_{\sigma\rho\nu_2}(k, -p_1 - p_3, -p_2) \gamma_{\rho\nu_1\nu_3}(p_1 + p_3, -p_1, -p_3) - \\ &-\frac{\tau_1}{p_{12}^2} \gamma_{\sigma\rho\nu_3}(k, -p_1 - p_2, -p_3) \gamma_{\rho\nu_1\nu_2}(p_1 + p_2, -p_1, -p_2) , \end{aligned} \quad (80)$$

where

$$\tau_1 = (12m)(3rm) , \tau_2 = (31m)(2rm) , \tau_3 = (23m)(1rm) , \tau_1 + \tau_2 + \tau_3 = 0 .$$

IV. CROSS SECTIONS FOR JET PRODUCTION IN QMRK

The typical process of the n -jet production in the quasi-multi-Regge kinematics is presented graphically at Fig. 1. Within this regime, one can use the Sudakov decomposition

$$q_i = \alpha_i P_B + \beta_i P_A + \mathbf{q}_{i\perp} , \quad \mathbf{q}_{i\perp} \cdot P_A = \mathbf{q}_{i\perp} \cdot P_B = 0 , \quad d^4 q_i = \frac{s}{2} d\alpha_i d\beta_i d^2 \mathbf{q}_i , \quad (81)$$

and the invariant masses of jets:

$$\begin{aligned} (P_A - q_1)^2 &= M_1^2 \approx -s\alpha_1 , \\ (q_1 - q_2)^2 &= M_2^2 \approx -s\alpha_2\beta_1 , \\ &\dots \\ (q_{n-2} - q_{n-1})^2 &= M_{n-1}^2 \approx -s\alpha_{n-1}\beta_{n-2} , \end{aligned}$$

$$(q_{n-1} + P_B)^2 = M_n^2 \approx s\beta_{n-1}, \quad (82)$$

by virtue of the ordering valid in the QMRK:

$$\alpha_1 \ll \alpha_2 \ll \dots \ll \alpha_n, \quad \beta_{n-1} \ll \beta_{n-2} \ll \dots \ll \beta_1, \quad M_i^2 \sim M^2 \ll s, \quad (83)$$

$$s_1 = (P_A - q_2)^2 \sim s_2 = (q_1 - q_3)^2 \sim \dots \sim s_{n-1} = (q_{n-2} + P_B)^2 \gg M^2. \quad (84)$$

Here M_i is the effective mass of the i -th jet. These quantities are related as $\Pi_1^{n-1} s_i = s \Pi_2^{n-1} M_i^2$.

The differential cross section of the n -jet production is given by

$$d\sigma^{2 \rightarrow n_{jet}} = \frac{1}{8s} |\mathcal{M}^{2 \rightarrow n}|^2 d\Gamma_n^{(jet)}. \quad (85)$$

The phase volume for the n jets containing n_i , $i = 1, \dots, n$ produced particles in each jet can be written as

$$d\Gamma_n^{(jet)} = \frac{(2\pi)^4}{s \cdot 2^{n-1}} \prod_{i=1}^{n-1} d^2 \mathbf{q}_i \prod_{i=1}^n d\phi_i \int_{\frac{M^2}{s}}^1 \frac{d\beta_1}{\beta_1} \int_{\beta_1}^1 \frac{d\beta_2}{\beta_2} \dots \int_{\beta_{n-3}}^1 \frac{d\beta_{n-2}}{\beta_{n-2}} = \frac{(2\pi)^4}{s \cdot 2^{n-1}} \prod_{i=1}^{n-1} d^2 \mathbf{q}_i \prod_{i=1}^n d\phi_i \cdot \frac{(\ln \frac{s}{M^2})^{n-2}}{(n-2)!}, \quad (86)$$

where

$$\begin{aligned} d\phi_1 &= dM_1^2 d\Gamma_1 (2\pi)^4 \delta^{(4)} \left(P_A - q_1 - \sum_{j=1}^{n_1} p_j^{(1)} \right), \\ d\phi_i &= dM_i^2 d\Gamma_i (2\pi)^4 \delta^{(4)} \left(q_{i-1} - q_i - \sum_{j=1}^{n_2} p_j^{(i)} \right), \quad i = 2, \dots, n-1, \\ d\phi_n &= dM_n^2 d\Gamma_n (2\pi)^4 \delta^{(4)} \left(q_{n-1} + P_B - \sum_{j=1}^{n_n} p_j^{(n)} \right), \end{aligned} \quad (87)$$

and

$$d\Gamma_i = \prod_{j=1}^{(n_i)} \frac{d^3 p_j^{(i)}}{2\varepsilon_j (2\pi)^3}. \quad (88)$$

Therefore, taking into account that the amplitude for $2 \rightarrow n$ production is given by

$$\mathcal{M}^{2 \rightarrow n} = 2^{-n+1} s \cdot g^n V_A V_B \left[\prod_{i=2}^{n-1} \frac{V_i^{i_1 \dots i_{n_i}}(q_i, q_{i+1})}{q_i^2} \right], \quad (89)$$

where $V_i(q_i, q_{i+1})$ are the RRP^{n_i} -vertices for n_i -particle production in i -th jet. The margin vertices defined as

$$V_A = \frac{1}{P_A^+} \Gamma_{\parallel}^{\rho\nu(i)-} e_\rho(p_A) \Pi e_{\nu_i}(p_i^{(1)}), \quad V_B = \frac{1}{P_B^-} \Gamma_{\parallel}^{\eta\nu(j)+} e_\eta(p_B) \Pi e_{\nu_j}(p_j^{(n)}). \quad (90)$$

For the case when jet consist from one particle and omitting the color factor we have

$$V_A = g(\Gamma^{\sigma\eta+}(P_A, q_2)/P_A^+) e_\sigma(P_A) e_\eta(P_{A'}) ; \quad \sum (V_A)^2 = 8g^2.$$

The differential cross section reads:

$$d\sigma^{2 \rightarrow n} = R(s) \alpha_s^n 2^{-5n+4} \pi^{-2n+3} \cdot V_A^2 V_B^2 \prod_{i=2}^{n-1} (V_i)^2 \cdot \frac{\prod_{i=1}^{n-1} d^2 \mathbf{q}_i}{\left(\prod_{i=1}^{n-1} q_i^2 \right)^2} \cdot \prod_{i=1}^n d\phi_i \frac{(\ln s/M^2)^{n-2}}{(n-2)!}, \quad (91)$$

where the intermediate gluons reggeization factor is included:

$$R(s) = \Pi_1^{n-1} (s_i/M^2)^{2(\omega(q_i^2)-1)}, \quad (92)$$

with M is some averaged value of jet invariant mass and $\omega(q^2)$, $\omega(0) = 1$ is the gluon Regge trajectory.

V. DISCUSSIONS AND CONCLUSIONS

The primary purpose of our investigation is to give a systematic self-consistent approach to derivation of the Feynman rules directly from the effective reggeon-particle action, and, what is essential, to present the results in a most convenient form for numerical simulations. We hope that our results will provide a practical help in writing relevant computer codes for phenomenological needs. In this work, we present the explicit expressions for effective vertices of the types $PR, RP, RPP, RRP, RRPP, RPPP, RRPPP, RPPPP$ derived directly within the framework of the effective Regge theory developed in the paper by one of us (L.N.L) [10]. Some of these vertices were obtained by means of different methods in Refs. [3, 11–13], while the two last vertices ($RRPPP$ and $RPPPP$) were not considered in literature up to now. All presented vertices satisfy the Bose-symmetry and gauge invariance conditions. Moreover, we made sure that the vertices of higher orders can be constructed, step by step, using the known ones given above.

The “nonlinear” vertices of type $RRRP$ with number of reggeons exceeding two can be constructed as well. We will not consider them here. The program of fitting the experimental data in QMRK using the effective vertices given above can be realized say for extracting the information about gluon reggeon parameters.

Acknowledgements

The work is partially supported by INTAS (Grant No. 00-00-366), RFBR (Grants Nos. 04-02-16445, 03-02-17077), and Russian Federation President’s Grant 1450-2003-2.

Appendix A

For convenience, we collect here several useful relations for vertices, which were derived and used in this work (here it is assumed that $k = p_1 + p_2 + p_3$):

$$p_1^\mu \gamma_{\rho\mu\lambda}(p_{13}, -p_1, -p_3) e^\lambda(p_3) = [p_{1\lambda} p_{13\rho} - g_{\lambda\rho} p_{13}^2] e^\lambda(p_3) , \quad (93)$$

$$p_{13}^\rho \gamma_{\sigma\rho\nu}(k, -p_{13}, -p_2) e^\nu(p_2) = [-k^2 g_{\nu\sigma} + k_\sigma p_{13\nu}] e^\nu(p_2), \quad (94)$$

$$p_{23}^\sigma \gamma_{\sigma\nu\lambda}(p_{23}, -p_2, -p_3) e^\nu(p_2) e^\lambda(p_3) = 0, \quad (95)$$

$$(p_1)^\mu \gamma_{\sigma\mu\rho}(k, -p_1, -p_{23}) = g_{\rho\sigma} [p_{23}^2 - k^2] + p_{1\sigma} p_{23\rho} + p_{1\rho} k_\sigma , \quad (96)$$

$$(q_1 - p_2)_\sigma \Gamma^{\sigma\nu-}(q_1, p_2 - q_1) e^\nu(p_2) = 0 . \quad (97)$$

Effective 4-gluon vertex has a property:

$$p_{1\nu_1} A_{r123}^{\sigma\nu_1\nu_2\nu_3} = k^2 \left[\frac{\tau_1}{p_{12}^2} p_1^{\nu_2} g^{\sigma\nu_3} - \frac{\tau_2}{p_{23}^2} \gamma^{\nu_2\nu_3\sigma}(-p_2, -p_3, p_{23}) - \frac{\tau_3}{p_{13}^2} p_1^{\nu_3} g^{\sigma\nu_2} \right] , \quad (98)$$

with

$$\tau_1 = (12m)(3rm) , \quad \tau_2 = (1rm)(23m) , \quad \tau_3 = (13m)(r2m) , \quad \sum \tau_i = 0 .$$

While checking the gauge invariance, the problem of cancellation of poles arises. They are cancelled due to identities listed below.

For the pole $1/p_{23}^2$ the relevant identity reads

$$\begin{aligned} & \sigma_1 C^\sigma(q_1, q_2) + \sigma_3 (n^-)_\rho \Gamma^{\rho\sigma+}(p_{23} - q_2, q_2) - \sigma_2 (n^+)_\rho \Gamma^{\rho\sigma-}(q_1, p_{23} - q_1) + \\ & p_{1\nu_1} [\gamma_{dr1e}^{-\sigma\nu_1+} + (n^-)_\rho \Delta_{dr1e}^{\rho\sigma\nu_1+} + (n^+)_\rho \Delta_{dr1e}^{-\sigma\nu_1\rho}] (q_1, p_{23}, p_1, q_2) = 0 , \end{aligned} \quad (99)$$

where we use

$$\sigma_1 = (edr)(1mr) , \quad \sigma_2 = (1er)(dmr) , \quad \sigma_3 = (d1r)(emr) , \quad \sum \sigma_i = 0 ,$$

and

$$\Delta_{dm1e}^{-\eta\sigma\nu_1}(q_1, p_{23}, p_1, q_2) = -q_1^2 \frac{(n^- n^- n^-)^{\sigma\nu_1\eta}}{p_1^-} \left[\frac{\sigma_2}{p_{23}} + \frac{\sigma_1}{q_2} \right],$$

$$\Delta_{dm1e}^{\rho\sigma\nu_1+}(q_1, p_{23}, p_1, q_2) = q_2^2 \frac{(n^+ n^+ n^+)^{\rho\sigma\nu_1}}{p_1^+} \left[\frac{\sigma_3}{p_{23}^+} + \frac{\sigma_1}{q_1^+} \right].$$

The compensation of the pole $1/p_{12}^2$ is provided by the relation:

$$Z_3 C^\sigma + Z_2 (n^-)_\rho \Gamma^{\rho\sigma+}(p_3 - q_2, q_2) - Z_1 (n^+)_\rho \Gamma^{\rho\sigma-}(q_1, p_3 - q_1) + p_{12\eta} [\gamma_{dm3e}^{-\eta\sigma+} + (n^-)_\rho \Delta_{dm3e}^{\rho\eta\sigma+} + (n^+)_\rho \Delta_{dm3e}^{-\eta\sigma\rho}] (q_1, p_{12}, p_3, q_2) = 0,$$

where we use $Z_1 = (3dr)(emr)$, $Z_2 = (e3r)(dmr)$, $Z_3 = (der)(3mr)$, $\sum Z_i = 0$, and

$$\Delta_{dr3e}^{-\eta\sigma\rho}(q_1, p_{12}, p_3, q_2) = -q_1^2 \frac{(n^- n^- n^-)^{\sigma\rho\eta}}{p_{12}^-} \left[\frac{Z_3}{q_2^-} + \frac{Z_1}{p_3^-} \right];$$

$$\Delta_{dr3e}^{\rho\eta\sigma+}(q_1, p_{12}, p_3, q_2) = q_2^2 \frac{(n^+ n^+ n^+)^{\rho\sigma\nu_1}}{p_{12}^+} \left[\frac{Z_3}{q_1^+} + \frac{Z_2}{p_3^+} \right].$$

The compensation of the pole $1/(p_1 - q_1)^2$ is provided by the relation:

$$\eta_2 (n^+)_\rho \gamma^{\nu_2\nu_3\rho}(-p_2, -p_3, p_{23}) + \eta_1 \Gamma^{\nu_2\nu_3+}(p_3 - q_2, q_2) - \eta_3 \Gamma^{\nu_3\nu_2+}(p_2 - q_2, q_2) + p_{23\rho} (\Delta + \gamma)_{m23e}^{\rho\nu_2\nu_3+}(q_1 - p_1, p_2, p_3, q_2) = 0,$$

with $\eta_1 = (3er)(2mr)$, $\eta_2 = (23r)(emr)$, $\eta_3 = (e2r)(3mr)$; $\sum \eta_i = 0$ and

$$\Delta_{m23e}^{\rho\nu_2\nu_3+}(q_1 - p_1, p_2, p_3, q_2) = -q_2^2 \frac{(n^+ n^+ n^+)^{\rho\nu_2\nu_3}}{p_{23}^+} \left[\frac{\eta_3}{p_{2+}} - \frac{\eta_1}{p_3^+} \right].$$

When compensating the pole $1/(p_2 - q_2)^2$ we use:

$$X_2 \Gamma^{\sigma\nu_3-}(q_1, p_{13} - q_1) + X_3 \Gamma^{\sigma\nu_3-}(q_1, p_3 - q_1) - X_1 (n^-)_\eta \gamma^{\eta\nu_3\sigma}(q_1 - p_1, -p_3, q_2 - p_2) + (p_1)_\rho (\Delta + \gamma)_{d13m}^{-\rho\nu_3\sigma}(q_1, p_1, p_3, q_2 - p_2) = 0,$$

with $X_1 = (d1r)(3mr)$, $X_2 = (13r)(dmr)$, $X_3 = (3dr)(1mr)$; $\sum X_i = 0$ and

$$\Delta_{d13m}^{-\rho\nu_3\sigma}(q_1, p_1, p_3, q_2 - p_2) = q_1^2 \frac{(n^- n^- n^-)^{\rho\nu_3\sigma}}{p_1^-} \left[\frac{X_3}{p_{3-}} + \frac{X_2}{p_{13}^-} \right].$$

When compensating the pole $1/(p_1 - q_2)^2$ we use:

$$-R_1 (n^-)_\rho \gamma^{\rho\nu_2\nu_3}(p_{23}, -p_2, -p_3) + R_2 \Gamma^{\nu_3\nu_2-}(q_1, p_2 - q_1) - R_3 \Gamma^{\nu_3\nu_2-}(q_1, p_3 - q_1) + (p_1 - q_2)_\rho (\Delta + \gamma)_{d23m}^{-\rho\nu_2\nu_3\rho}(q_1, p_2, p_3, q_2 - p_1) = 0,$$

with $R_1 = (23r)(dmr)$, $R_2 = (d2r)(3mr)$, $R_3 = (3dr)(2mr)$; $\sum R_i = 0$ and

$$\Delta_{d23m}^{-\nu_2\nu_3\rho}(q_1, p_2, p_3, q_2 - p_1) = q_1^2 \frac{(n^- n^- n^-)^{\nu_2\nu_3\rho}}{p_{23}^-} \left[\frac{R_3}{p_3^-} - \frac{R_2}{p_2^-} \right].$$

When compensating the pole $1/(p_2 - q_1)^2$ we use:

$$-Y_1 \Gamma^{\rho\nu_3+}(p_{13} - q_2, q_2) - Y_3 \Gamma^{\rho\nu_3+}(p_3 - q_2, q_2) - Y_2 (n^+)_\sigma \gamma^{\rho\nu_3\sigma}(q_1 - p_2, -p_3, q_2 - p_1) - (p_1)_\eta (\Delta + \gamma)_{m13e}^{\rho\eta\nu_3+}(q_1 - p_2, p_1, p_3, q_2) = 0,$$

with $Y_1 = (13r)(emr)$, $Y_2 = (e1r)(3mr)$, $Y_3 = (3er)(1mr)$; $\sum Y_i = 0$ and

$$\Delta_{m13e}^{\rho\eta\nu_3+}(q_1 - p_2, p_1, p_3, q_2) = q_2^2 \frac{(n^+ n^+ n^+)^{\rho\eta\nu_3}}{p_1^+} \left[\frac{Y_1}{p_{13}^+} + \frac{Y_3}{p_3^+} \right].$$

In testing the gauge properties of margin vertices a new identity appears:

$$x_1 \gamma^{\nu_2\nu_3\rho}(-p_2, -p_3, p_{23}) + x_2 \gamma^{\nu_3\rho\nu_2}(p_2 - P_A, P_A, -p_2) - x_3 \gamma^{\nu_2\rho\nu_3}(p_3 - P_A, P_A, -p_3) + \gamma_{d23r}^{\rho\nu_2\nu_3\sigma}(p_1 - q_2)_\sigma = 0, \quad (100)$$

with

$$x_1 = (32m)(drm), \quad x_2 = (2dm)(3rm), \quad x_3 = (d3m)(2rm), \quad x_1 + x_2 + x_3 = 0. \quad (101)$$

Besides this, the relation (the generalized Jacobi identity, which is a consequence of the ordinary Jacobi ones) arises for combinations of the structure constants when compensating of γ terms:

$$(1em)(d2r)(m3r) - (13r)(2dm)(erm) - (rd1)(r2m)(e3m) + (12r)(e3m)(drm) = 0, \quad (102)$$

what leads to

$$(m1e)\gamma_{d23m}^{-\nu_2\nu_3+} + (m1d)\gamma_{m23e}^{-\nu_2\nu_3+} + (m12)\gamma_{dm3m}^{-\nu_2\nu_3+} + (m13)\gamma_{d2me}^{-\nu_2\nu_3+} = 0. \quad (103)$$

Appendix B

In the paper by one of us (L.N.L), Ref. [10], the recurrence relation was derived for induced vertices that allows one to build vertices of higher orders provided that the lower ones are known.

It is convenient to introduce the simplified definitions

$$\begin{aligned}\Delta_{ca_1, \dots, a_n, d}^{\rho\nu_1 \dots \nu_n +}(k_0, k_1, \dots, k_n, q_2) &= q_2^2 (n^+)^{\rho} (n^+)^{\nu_1} \dots (n^+)^{\nu_n} d_{ca_1, \dots, a_n, d}^{(n)+}(q_1, p_1, \dots, p_n) ; \\ \Delta_{ca_n, \dots, a_1, d}^{-\nu_n \dots \nu_1 \eta}(q_1, k_n, \dots, k_1, k_0) &= q_1^2 (n^-)^{\eta} (n^-)^{\nu_1} \dots (n^-)^{\nu_n} d_{ca_n, \dots, a_1, d}^{(n)-}(p_n, \dots, p_1, q_2) ,\end{aligned}\tag{104}$$

with the conservation laws:

$$q_1^+ = (p_1 + \dots + p_n)^+ ; \quad q_2^- = (p_1 + \dots + p_n)^- .$$

The lowest order expressions are:

$$d_{cad}^{(1)+} = \frac{1}{p_1^+} (cad) ; \quad d_{cad}^{(1)-} = -\frac{1}{p_1^+} (cad) .\tag{105}$$

The recurrence relations are given by

$$\begin{aligned}d_{c1 \dots nd}^{(n)+}(q_1, p_1, \dots, p_n) &= \frac{1}{p_n^+} \left[(mnc) d_{m1 \dots (n-1)d}^{(n-1)+}(q_1 - p_n, p_1, \dots, p_{n-1}) + \right. \\ &\left. (mn1) d_{cm2 \dots (n-1)d}^{(n-1)+}(q_1, p_{1n}, p_2, \dots, p_{n-1}) + \dots + (mn(n-1)) d_{c1 \dots (n-2)md}^{(n-1)+}(q_1, p_1, \dots, p_{n-2}, p_{n-1} + p_n) \right] ,\end{aligned}\tag{106}$$

and

$$\begin{aligned}d_{cn \dots 1d}^{(n)-}(p_n, \dots, p_1, q_2) &= \frac{1}{p_n^-} \left[(mnd) d_{c(n-1) \dots 1m}^{(n-1)-}(p_{n-1}, \dots, p_1, q_2 - p_n) + \right. \\ &\left. (mn1) d_{c(n-1) \dots 2md}^{(n-1)-}(p_{n-1}, \dots, p_1 + p_n, q_2) + \dots + (mn(n-1)) d_{cm(n-2) \dots 1d}^{(n-1)-}(p_{n-1} + p_n, p_{n-2}, \dots, p_1, q_2) \right] .\end{aligned}\tag{107}$$

The induced vertices of the rank-2 read

$$d_{c12d}^{(2)+}(q_1, p_1, p_2) = \frac{1}{p_2^+} \left(\frac{T_1}{q_1^+} + \frac{T_2}{p_1^+} \right) = \frac{1}{p_1^+} \left(-\frac{T_3}{p_2^+} - \frac{T_1}{p_1^+} \right) = \frac{1}{q_1^+} \left(\frac{T_2}{p_1^+} - \frac{T_3}{p_2^+} \right) ,\tag{108}$$

$$T_1 = (21m)(dcm) , \quad T_2 = (1dm)(2cm) , \quad T_3 = (d2m)(1cm) , \quad T_1 + T_2 + T_3 = 0 ; \quad q_1^+ = p_1^+ + p_2^+ ,$$

and

$$d_{c21d}^{(2)-}(p_2, p_1, q_2) = \frac{1}{p_2^-} \left(-\frac{T_1}{q_2^-} - \frac{T_3}{p_1^-} \right) = \frac{1}{p_1^-} \left(\frac{T_1}{q_2^-} + \frac{T_2}{p_2^+} \right) = \frac{1}{q_2^-} \left(\frac{T_2}{p_2^-} - \frac{T_3}{p_1^-} \right) , \quad q_2^- = p_1^- + p_2^- ,\tag{109}$$

and with the same definitions for T_i 's.

Quantities $d^{(n)\pm}$ have the Bose-symmetry properties: namely they are invariant relative to simultaneous replacements of Lorentz and color indices and the momenta of any pair of particles.

-
- [1] V.S. Fadin, E.A. Kuraev, L.N. Lipatov, Phys. Lett. **B60** (1975) 50; E.A. Kuraev, L.N. Lipatov, V.S. Fadin, Zh. Eksp. Teor. Fiz. **71** (1976) 840 [Sov. Phys. JETP **44** 443 (1976)]; *ibid.* **72** (1977) 377 [**45** (1977) 199]; I.I. Balitsky, L.N. Lipatov, Yad. Fiz. **28** (1978) 1597 [Sov. J. Nucl. Phys. **28** (1978) 822].
- [2] M. Derrick *et al.* [ZEUS Collaboration], Phys. Lett. B **B345** (1995) 576; C. Adloff *et al.* [H1 Collaboration], Eur. Phys. J. **C21** (2001) 33; S. Chekanov *et al.* [ZEUS Collaboration], Eur. Phys. J. **C21** (2001) 443.
- [3] L.N. Lipatov, V.S. Fadin, JETP Lett. **49** (1989) 352; Yad. Fiz. **50** (1989) 1141.
- [4] V.S. Fadin, L.N. Lipatov, Phys. Lett. **B429** (1998) 127.

- [5] M. Ciafaloni, G. Camici, Phys. Lett. **B430** (1998) 349.
- [6] A.H. Mueller, Phys. Lett. **B396** (1997) 251.
- [7] L.D. McLerran, R. Venugopalan, Phys. Rev. **D50** (1994) 2225.
- [8] V.T. Kim, G.B. Pivovarov, Phys. Rev. Lett. **79** (1997) 809.
- [9] L.N. Lipatov, Nucl. Phys. **B365** (1991) 614; R. Kirschner, L.N. Lipatov, L. Szymanowski, Nucl. Phys. **B425** (1994) 579.
- [10] L.N. Lipatov, Nucl. Phys. **B452** (1995) 369.
- [11] V.S. Fadin, L.N. Lipatov, Nucl. Phys. **B477** (1996) 767.
- [12] L.N. Lipatov, Phys. Rept. **286** (1997) 131.
- [13] A. Leonidov, D. Ostrovsky, Phys. Rev. D **62** (2000) 094009.
- [14] J. Schwarz, Phys. Reports **89** (1982) 223; E.N. Antonov, Preprint PNPI-1808 (1992).
- [15] O. Nachtmann, Annals Phys. **209** (1991) 436.
- [16] H. Verlinde, E. Verlinde, hep-th/9302104.
- [17] I. Balitsky, Nucl. Phys. **B463** (1996) 99; Phys. Rev. **D60** (1999) 014020.
- [18] Y.V. Kovchegov, Phys. Rev. **D60** (1999) 034008; Phys. Rev. **D61** (2000) 074018.

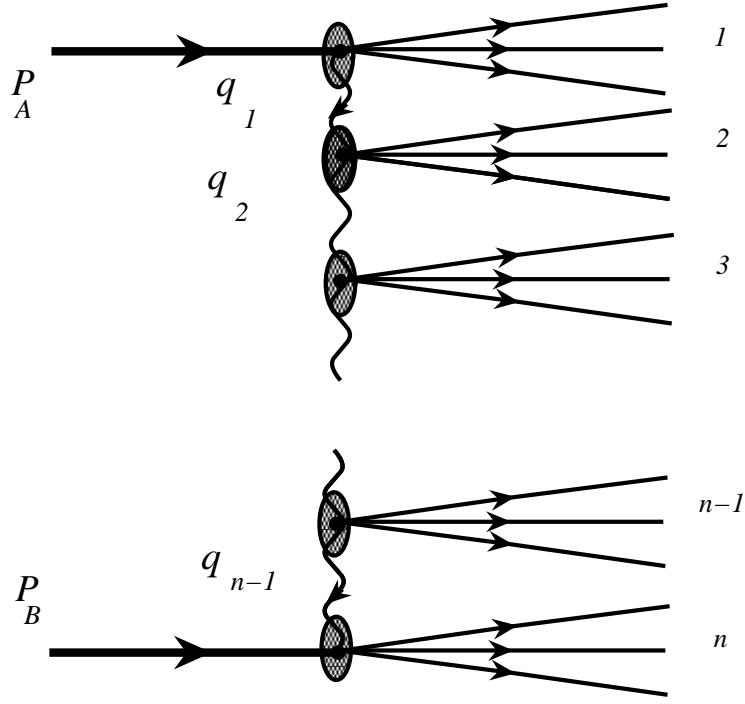


FIG. 1: Quasi-multi-Regge kinematics: notations. Process of n -jet production $2 \rightarrow n_{jets}$ in the quasi-multi-Regge kinematics.

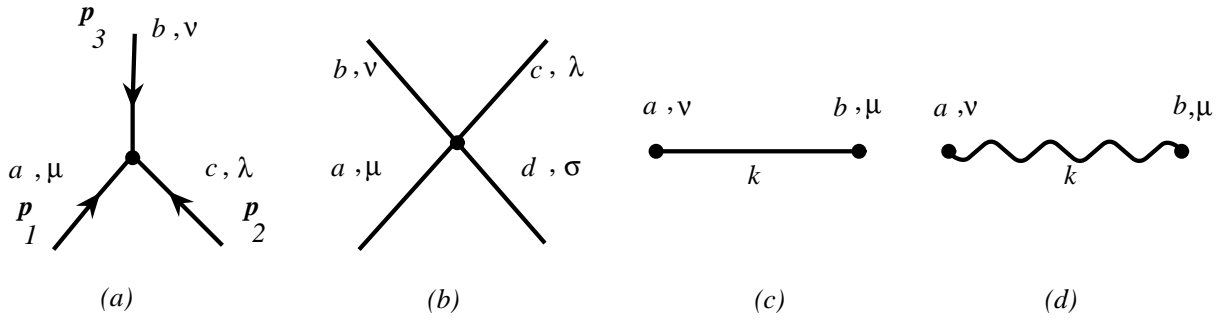


FIG. 2: Standard QCD Feynman rules: vertices (a-c), and the reggeized gluon propagator (d).

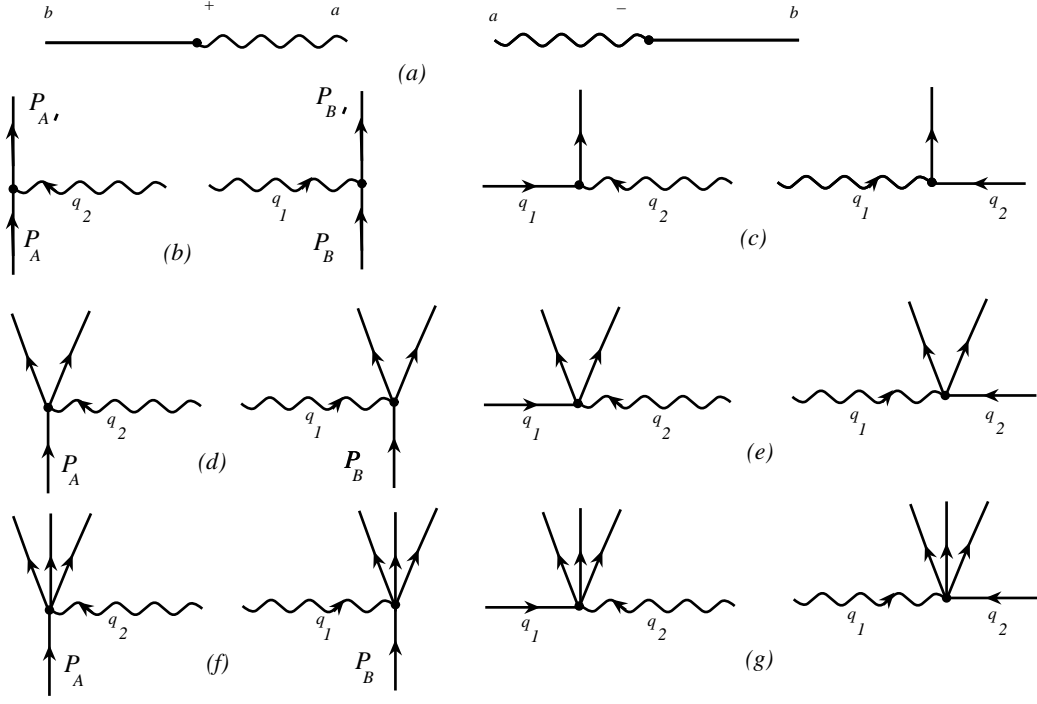


FIG. 3: List of the induced vertices.

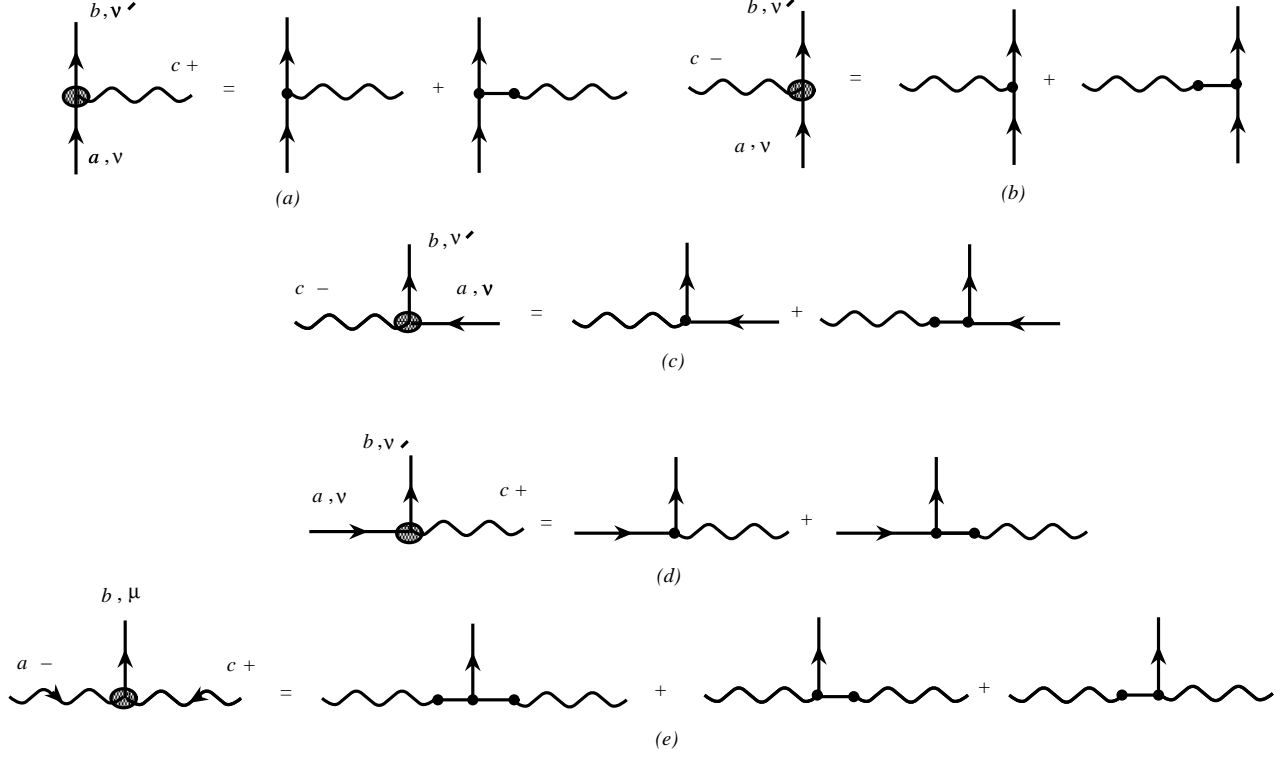


FIG. 4: PPR (a-d) and RRP (e) effective vertices.

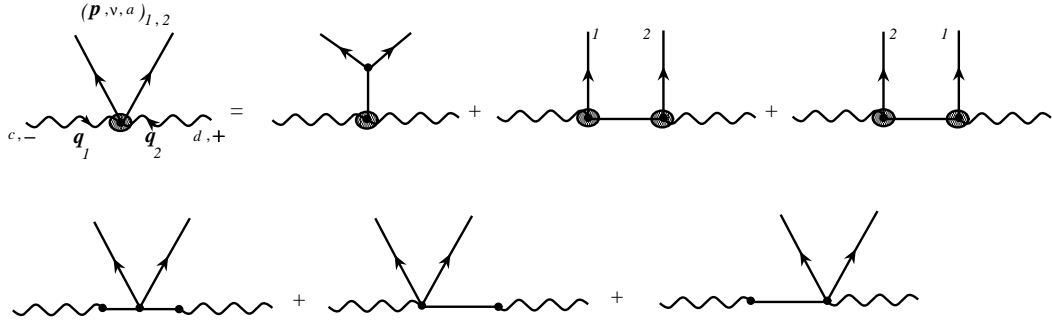


FIG. 5: Central *PPRR* effective vertex.

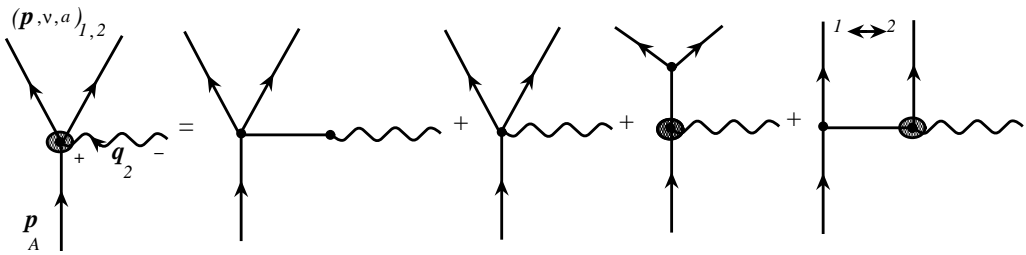


FIG. 6: Margin *PPPR* effective vertex: “left” type.

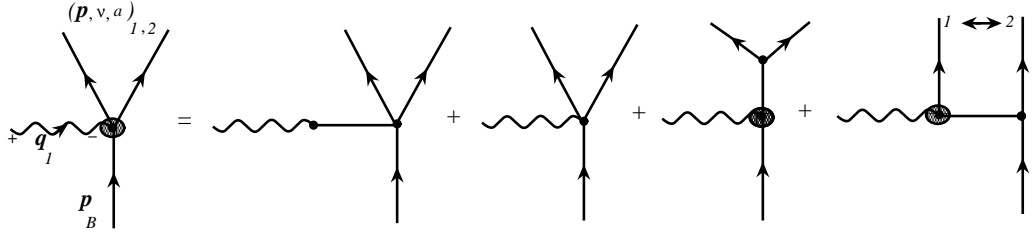


FIG. 7: Margin *PPR* effective vertex: “right” type.

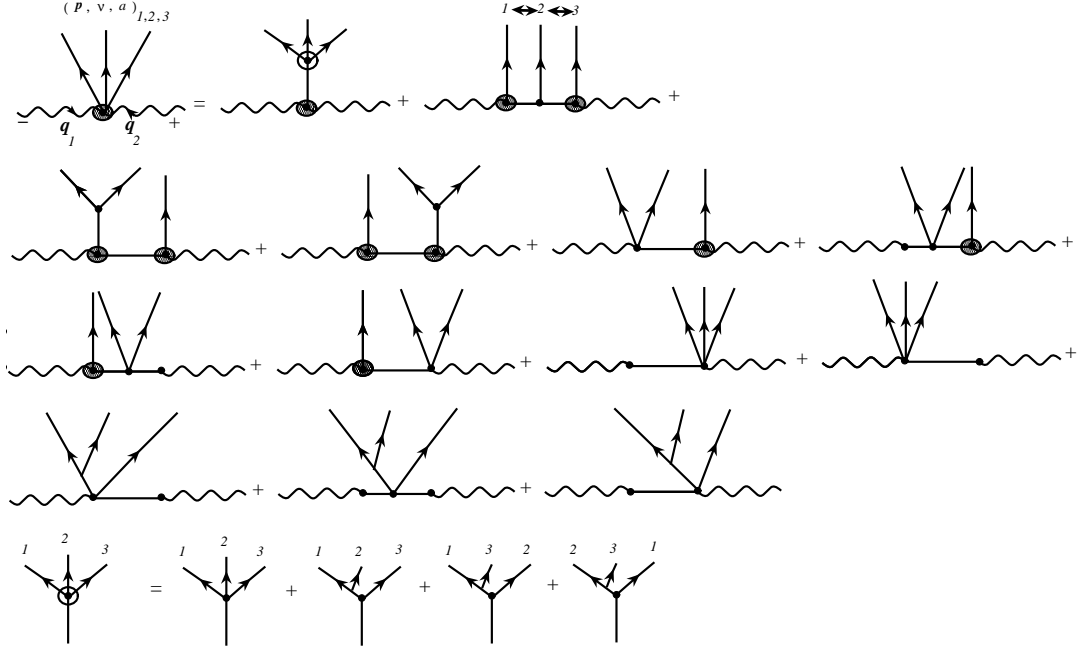


FIG. 8: Central *RRPPP* effective vertex.

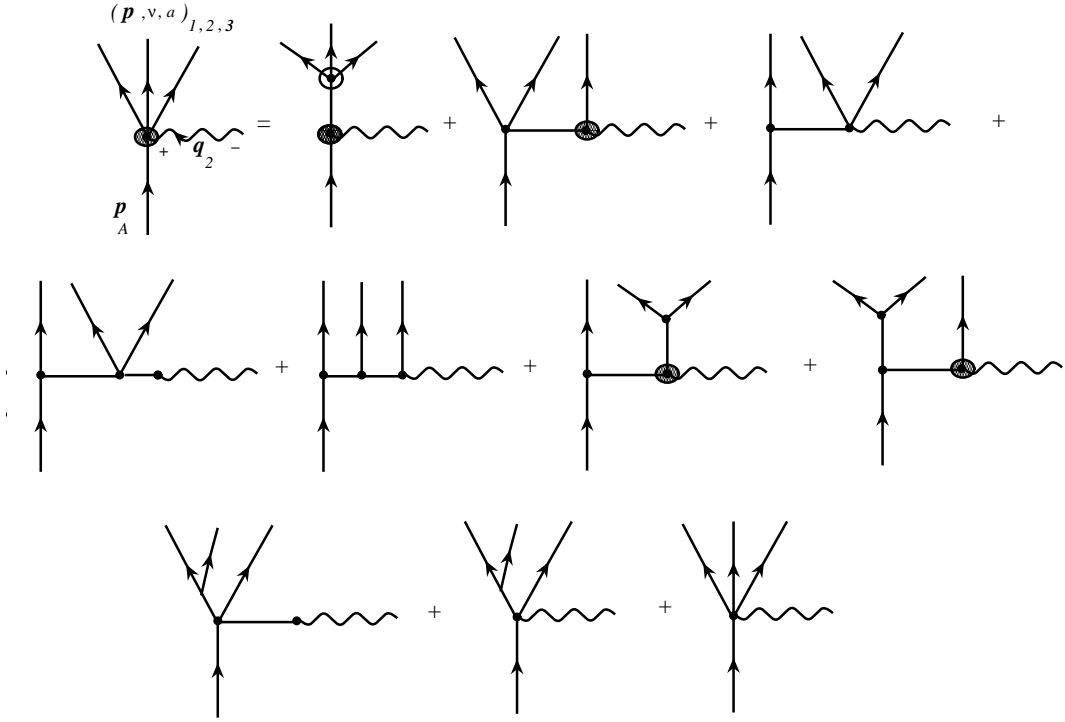


FIG. 9: Margin *PPPR* effective vertex: “left” type.

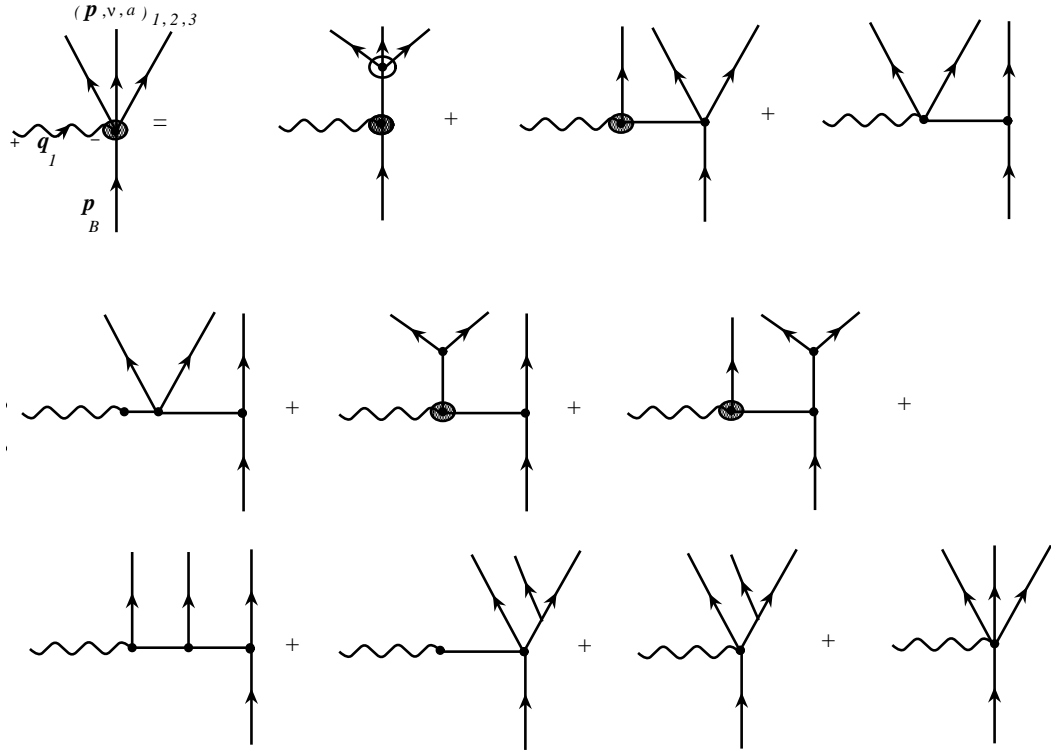


FIG. 10: Margin *PPPR* effective vertex: “right” type.

(Dated: January 27, 2020)

Abstract

